



Ball End Mill—Tool Radius Compensation of Complex NURBS Surfaces for 3-Axis CNC Milling Machines

Zhaoqin Wang^{1,2,3} · Xiaorong Wang^{1,2} · Yusen Wang¹ · Ruijun Wang⁴ · Manyu Bao⁴ · Tiesong Lin⁵ · Peng He⁵

Received: 10 May 2019 / Revised: 11 March 2020 / Accepted: 31 March 2020 / Published online: 20 May 2020
© Korean Society for Precision Engineering 2020

Abstract

In order to extend the 2D-TRC (tool radius compensation) function of 3-axis CNC milling machines to ball end mills (BEMs), a new TRC named BEM-TRC is proposed to achieve successful milling of complex surfaces without over-cut. The implementation of the BEM-TRC for complex surfaces depicted in NURBS model is divided into three steps. The first one is to search the cutting point (CP) on a NURBS surface using equi-arc length interpolation in u or v direction. The second one is to accomplish BEM-TRC at the CP through offsetting the CP to the cutter center point (CCP) of a BEM along the normal vector at CP. The third one is to compute the cutter location point (CLP) of the BEM according to the BEM-CCP. The simulation and experiment verifies that the BEM-TRC is feasible and effective, and can avoid over-cut phenomenon successfully. The BEM-TRC extends the ability of the traditional 2D-TRC function, and makes 3-axis CNC milling machines to accomplish the milling process of complex NURBS surfaces.

Keywords NURBS surface · Ball end mill · Tool radius compensation · 3-Axis CNC milling machines

1 Introduction

The non-uniform rational B-splines (NURBS) model provides researchers with an exact uniform representation of analytical shapes as well as free-form parametric curves and surfaces [1–3]. Due to the advantages of NURBS, STEP-NC has adopted NURBS as the standard interface for data exchange between CAD/CAM and CNC systems [4, 5]. The

NURBS model endows researchers to design a large variety of shapes by operating the control points as well as weights in a flexible way owing to its generality in the expression of complex curves and surfaces [6]. Many CNC system manufacturers devote themselves to developing NURBS interpolators for their CNC systems. Unfortunately, except for few expensive CNC systems, common 3-axis CNC milling machines are equipped with only linear interpolation (G01) and circular interpolation (G02/G03) without NURBS interpolation [7]. How to realize the NURBS interpolation oriented to 3-axis CNC milling machines is still an urgent problem to be solved for such level machines.

Owing to low-cost and flexibility, 3-axis CNC milling machines have been utilized in many industries such as aerospace, ships, die module and automobiles [8]. As a basic and essential function, such level CNC milling machines are equipped with the 2D tool radius compensation (2D-TRC). Except for few CNC systems equipped with 3D-TRC function (such as Mitsubishi CNC 330M/330HM/335M in Japan, Maho CNC432 in Germany, etc.), [9–11] almost all 3-axis CNC milling machines are equipped with 2D-TRC function which can meet the machining demands for most of planar contours. The 2D-TRC makes the programming procedure to be an easy task for the reason that programmers accomplish programming according to the actual contour of parts without considering

✉ Zhaoqin Wang
wzqpapers@126.com

✉ Xiaorong Wang
wxrlanzhou@126.com

¹ School of Mechatronic Engineering, Lanzhou Jiaotong University, Lanzhou 730010, China

² Key Laboratory of System Dynamics and Reliability of Rail Transport Equipment of Gansu Province, Lanzhou Jiaotong University, Lanzhou 730010, China

³ State Key Laboratory of Advanced Processing and Recycling of Nonferrous Metals, Lanzhou University of Technology, Lanzhou 730050, China

⁴ Beijing JinLunKunTian Special Machine Co. LTD., Beijing 100083, China

⁵ State Key Laboratory of Advanced Welding and Joining, Harbin Institute of Technology, Harbin 150001, China

the actual tool paths. However, the 2D-TRC function has some disadvantages as follows:

- (1) The 2D-TRC function is only suitable for flat end mills (FEMs), while is unsuitable for ball end mills (BEMs).
- (2) The 2D-TRC function can be only able to cut the planar contours, while be unable to cut complex spatial surfaces.

With the development of machining, complex surfaces have been more and more commonly used in various industries [12–15]. Such complex surfaces can be machined based on 5-axis CNC milling machines using many CAM software such as UG, CATIA, ProE and PowerMill [16–19]. However, a lot of companies can't afford such expensive 5-axis CNC milling machines. Accomplishing the machining of complex surfaces using 3-axis CNC milling machines becomes a practical and cheap choice for many manufacturing enterprises. The CNC milling of complex NURBS surfaces using BEMs has been still a challenge for common 3-axis milling machines equipped with 2D-TRC function and without NURBS interpolation function. In this work, the BEM-TRC of complex NURBS surfaces for 3-axis CNC milling machines is proposed in order to overcome the conundrum. The algorithm, principle and application are discussed in detail. The following goals will be pursued for common 3-axis milling machines: (1) to extend the 2D-TRC function to be applied to BEMs, (2) to explore new TRC method for the milling of NURBS complex surfaces, and (3) to investigate the interpolation method for NURBS complex surfaces with BEM-TRC.

2 NURBS Surface Representation and Its Partial Derivatives

In modern CAD/CAM systems, parts with complex surfaces (e.g. aircraft models, blades, and module dies) are generally expressed in parametric surfaces. In parametric surfaces, NURBS models are becoming more and more important and widely used in the CAD and CAM communities because they offer an exact uniform representation of both analytical and free-form parametric curves and surfaces. As a result, complex surfaces are described by the NURBS model in this work.

A NURBS surface is a bivariate vector-valued piecewise rational function. A $p \times q$ degree NURBS surface can be expressed as follows [20]:

$$S(u, v) = \frac{\sum_{i=0}^n \sum_{j=0}^m N_{i,p}(u)N_{j,q}(v)w_{i,j}P_{i,j}}{\sum_{i=0}^n \sum_{j=0}^m N_{i,p}(u)N_{j,q}(v)w_{i,j}} \quad (0 \leq u, v \leq 1) \tag{1}$$

where $\{P_{i,j}\}$ form a bidirectional control point net, $\{w_{i,j}\}$ are the weights, and $\{N_{i,p}(u)\}$ and $\{N_{j,q}(v)\}$ are called p th and q th degree basis functions, respectively. With $\{N_{i,p}(u)\}$ as an example, its recursive formulae is written as:

$$\begin{cases} N_{i,0}(u) = \begin{cases} 1 & \text{for } u_i \leq u < u_{i+1} \\ 0 & \text{otherwise} \end{cases} \\ N_{i,p}(u) = \frac{u-u_i}{u_{i+p}-u_i}N_{i,p-1}(u) + \frac{u_{i+p+1}-u}{u_{i+p+1}-u_{i+1}}N_{i+1,p-1}(u) \\ \text{defined}_0^0 = 0 \end{cases} \tag{2}$$

$\{N_{i,p}(u)\}$ and $\{N_{j,q}(v)\}$ are the nonrational B-spline basis functions defined on U and V , respectively. The knot vectors of U and V are presented as:

$$U = \left\{ \underbrace{0, \dots, 0}_{p+1}, u_{p+1}, \dots, u_{r-p-1}, \underbrace{1, \dots, 1}_{p+1} \right\} \quad (r = n + p + 1) \tag{3}$$

$$V = \left\{ \underbrace{0, \dots, 0}_{q+1}, u_{q+1}, \dots, u_{s-q-1}, \underbrace{1, \dots, 1}_{q+1} \right\} \quad (s = m + q + 1) \tag{4}$$

Furthermore, the piecewise rational basis function of $\{R_{i,j}(u, v)\}$ can be defined as follows:

$$R_{i,j}(u, v) = \frac{N_{i,p}(u)N_{j,q}(v)w_{i,j}}{\sum_{k=0}^n \sum_{l=0}^m N_{k,p}(u)N_{l,q}(v)w_{k,l}} \quad (0 \leq u, v \leq 1) \tag{5}$$

As a result, Eq. (1) can be rewritten as:

$$S(u, v) = \sum_{i=0}^n \sum_{j=0}^m R_{i,j}(u, v)P_{i,j} \tag{6}$$

Assuming that:

$$S(u, v) = \frac{w(u, v)S(u, v)}{w(u, v)} = \frac{A(u, v)}{w(u, v)} \tag{7}$$

The derivative of $S(u, v)$ can be computed as follows:

$$\begin{aligned} S_\alpha(u, v) &= \frac{A_\alpha(u, v)w(u, v) - A(u, v)w_\alpha(u, v)}{w^2(u, v)} \\ &= \frac{A_\alpha(u, v)w(u, v) - S(u, v)w(u, v)w_\alpha(u, v)}{w^2(u, v)} \\ &= \frac{A_\alpha(u, v) - S(u, v)w_\alpha(u, v)}{w(u, v)} \end{aligned} \tag{8}$$

here α denotes u or v .

$A^{(k,l)}$ can be calculated using Eq. (9):

$$\begin{aligned}
 A^{(k,l)} &= [(wS)^k]^l = \left(\sum_{i=0}^k C_k^i w^{(i,0)} S^{(k-i,0)} \right)^l \\
 &= \sum_{i=0}^k C_k^i \sum_{j=0}^l C_l^j w^{(i,j)} S^{(k-i,l-j)} \\
 &= w^{(0,0)} S^{(k,l)} + \sum_{i=1}^k C_k^i w^{(i,0)} S^{(k-i,l)} + \sum_{j=1}^l C_l^j w^{(0,j)} S^{(k,l-j)} \\
 &\quad + \sum_{i=1}^k C_k^i \sum_{j=1}^l C_l^j w^{(i,j)} S^{(k-i,l-j)}
 \end{aligned}
 \tag{9}$$

So, $S^{(k,l)}$ can be expressed as follows:

$$\begin{aligned}
 S^{(k,l)} &= \frac{1}{w} \left(A^{(k,l)} - \sum_{i=1}^k C_k^i w^{(i,0)} S^{(k-i,l)} \right. \\
 &\quad \left. - \sum_{j=1}^l C_l^j w^{(0,j)} S^{(k,l-j)} - \sum_{i=1}^k C_k^i \sum_{j=1}^l C_l^j w^{(i,j)} S^{(k-i,l-j)} \right)
 \end{aligned}
 \tag{10}$$

where

$$\frac{\partial^{k+l}}{\partial^k u \partial^l v} A(u, v) = \sum_{i=0}^n \sum_{j=0}^m N_{i,p}^k N_{j,q}^l P_{ij}^w \quad (P^w = wP)
 \tag{11}$$

$$\frac{\partial^{k+l}}{\partial^k u \partial^l v} w(u, v) = \sum_{i=0}^n \sum_{j=0}^m N_{i,p}^k N_{j,q}^l w_{1_{ij}} \quad (w_1 = w)
 \tag{12}$$

3 Principle of BEM-TRC for NURBS Surfaces

3.1 The Principle of BEM-TRC

In the milling of a NURBS surface employing a BEM, the over-cut phenomenon will happen when the TRC function is not utilized during programming. The over-cut is inevitable when a CNC program controls the cutter location point (CLP) of a BEM to run along a predefined tool path. This is why the TRC function is vital in the CNC milling process. Oriented to 3-axis CNC milling machines, the TRC can be carried out by offsetting a point S on a NURBS surface one R distance (R is the radius of a BEM) along its normal vector n (as shown in Fig. 1a) under the condition that the cutter shaft can not be changed.

The tangent vectors of τ_u and τ_v at the S point (as shown in Fig. 1a) can be calculated as follows:

$$\tau_u = S_u(u, v)
 \tag{13}$$

$$\tau_v = S_v(u, v)
 \tag{14}$$

here τ_u and τ_v are the tangent vectors in u and v directions, respectively. Hence, the normal vector of S point can be written as follows:

$$n = \tau_u \times \tau_v = S_u(u, v) \times S_v(u, v)
 \tag{15}$$

A milling method of a NURBS surface can be performed by controlling the cutter to move in v or u direction. For example, the milling process can be carried out through controlling the cutter to cut materials along a NURBS curve (in

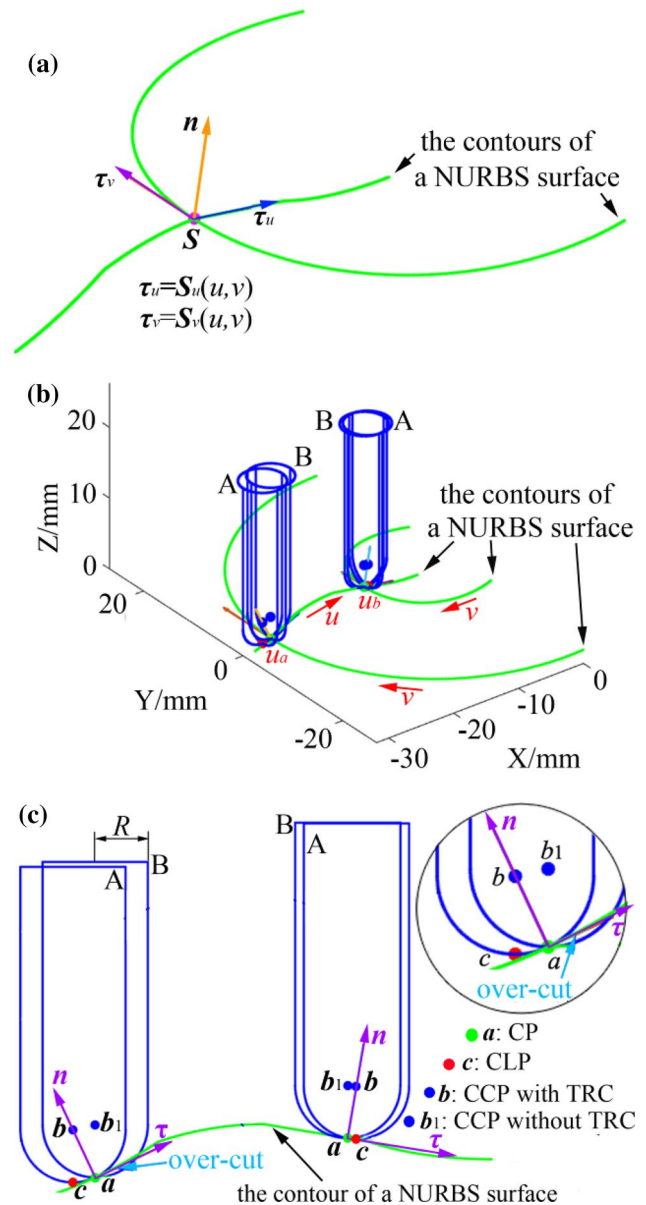


Fig. 1 The milling procedure and BEM-TRC of a NURBS surface, **a** normal vector calculation of a point on a NURBS surface, **b** the schematic of the milling procedure of a NURBS surface, **c** the milling procedure with/without BEM-TRC

v direction, $0 \leq v \leq 1$) on the NURBS surface using a specific u value (as shown in Fig. 1b).

The milling of a NURBS surface can be considered as the comprehensive cutting effect of many NURBS curves on the surface. As a result, the milling of a NURBS curve is the milling basis of the corresponding NURBS surface. Figure 1c shows the schematic of the milling procedure for a NURBS curve using a BEM with and without TRC. When a BEM cuts a NURBS curve without using the TRC function, the CNC program will manipulate the CLP c of the cutter to move along the NURBS curve. For example, when a BEM cuts the cutting point (CP) a on the NURBS surface, the CNC program will manipulate the BEM-CLP to cut the CP a . This makes the CNC program to manoeuvre the cutter to locate the B position (as shown in Fig. 1c). It will lead to over-cut phenomenon inevitably due to the non-zero curvature at the CP a . Adjusting the pose of the cutter can avoid the over-cut phenomenon successfully. Unfortunately, 3-axis CNC milling machines are unable to realize the pose adjustment of the cutter. Consequently, offsetting the cutter at the CP a is the only feasible way to avoid over-cut phenomenon.

In order to perform the BEM-TRC function, the CP a should be offset one R distance to the CCP b along its normal vector n as shown in Fig. 1c. The CCP b of the cutter can be computed as follows:

$$b = S + Rn \tag{16}$$

here R is the radius of the BEM.

Then the CLP of the cutter can be calculated according to the CCP b . This makes the cutter to locate to the position A (as shown in Fig. 1c). Thus, a CNC program can be generated according to the CLP c of the cutter, which can be obtained as follows:

$$c = b - R[0 \ 0 \ 1] \tag{17}$$

This makes the hemisphere of the BEM to be tangent to the NURBS surface at the CP a . Hence, the over-cut phenomenon can be avoided accordingly.

3.2 The Interpolation and Accuracy Control for BEM-TRC

Figure 2 shows the point cloud model of a NURBS surface. Its control point (P), weight (w), knot vectors (U and V) and degree ($p \times q$) are defined as outlined in Appendix A.

In order to accomplish the milling of the NURBS surface (as shown in Fig. 2) using the BEM-TRC function. The complete procedure includes three steps:

- (1) The CPs on the NURBS surface are computed using the equi-arc length interpolation (EALI) meeting the precision requirement. Based on our previous research

on NURBS interpolation, the EALI can be realized by employing the fixed step plus golden section interpolation (FS + GSI) [21].

- (2) The BEM-TRC is executed at the CPs of the NURBS surface.
- (3) The BEM-CLP is computed according to the BEM-CCP.

Summarily, the flowchart of the BEM-TRC function for NURBS surfaces based on 3-axis CNC milling machines is illustrated in Fig. 3.

Figure 4 shows the tool paths and milling effects of the NURBS surface (as shown in Fig. 2) with BEM-TRC using various (s_u, s_v) values. As can be observed in Fig. 4, the distribution of interpolation points is even along NURBS curves when the EALI method is employed, and the interpolation precision can be controlled well. Additionally, the smaller the assigned arc length s is, the better approximation of tool paths to the contours of the NURBS surface can be obtained.

When the expected arc length s is assigned, an important problem is whether the error between the actual arc length s_i and the assigned arc length s can reach the desired accuracy. Figure 5 shows that the s_i - s curves lay inside the range of $[-1 \ 1] \times 10^{-3}$, which meets the milling accuracy requirement.

Figure 6 illustrates the paths of BEM-CLP with and without BEM-TRC. Apparently, paths without BEM-TRC don't coincide with those of BEM-TRC. The red paths are NURBS curves on the NURBS surface corresponding to explicit u values. When the milling is performed without BEM-TRC, the BEM-CLP follows the red paths and the over-cut phenomenon happens. If the over-cut phenomenon is avoided, the BEM-CLP have to move along the green paths. Accordingly, it makes the BEM-CP to move along the red curves. Thus, the paths of the BEM-CLP (BEM-CP) deviate from (coincide with) the NURBS curves to be cut, respectively.

In the interpolation researches, the interpolation accuracy is a matter of great concern. When a line segment sequence approaches a NURBS curve, the chord d can denote the interpolation accuracy and be calculated as follows [22]:

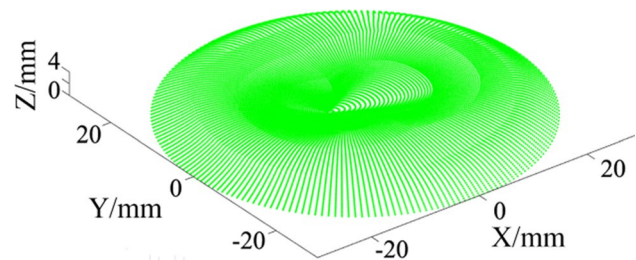


Fig. 2 The point cloud model of a NURBS surface

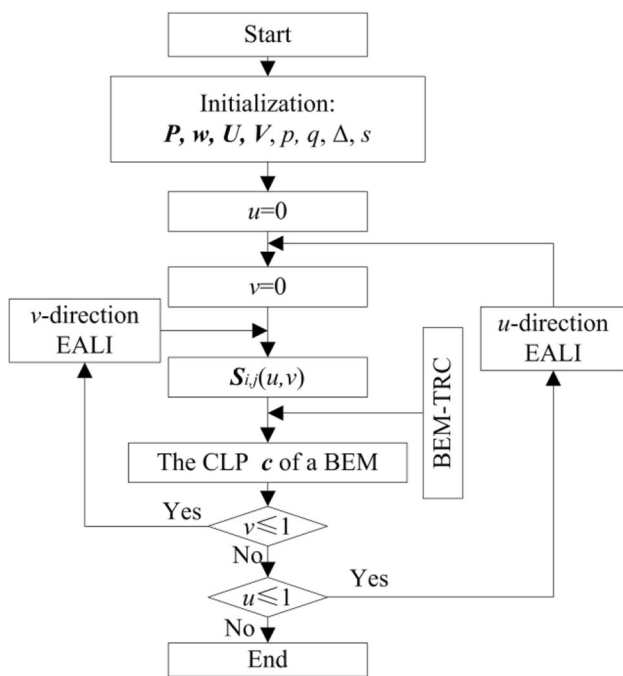


Fig. 3 The flowchart of the BEM-TRC function for NURBS surfaces based on 3-axis CNC milling machines (Δ is fixed step, s is assigned arc length)

$$d = \frac{|I \times C_x(u_i) + J \times C_y(u_i) + K|}{\sqrt{I^2 + J^2}} \tag{18}$$

here

$$u_t = (u_i + u_{i+1})/2$$

$$Ix + Jy + K = 0$$

$$I = \frac{1}{C_x(u_{i+1}) - C_x(u_i)}$$

$$J = -\frac{1}{C_y(u_{i+1}) - C_y(u_i)}$$

$$K = -\frac{C_x(u_i)}{C_x(u_{i+1}) - C_x(u_i)} + \frac{C_y(u_i)}{C_y(u_{i+1}) - C_y(u_i)}$$

According to Eq. (18), the chord d curves of $s = 1$ mm and 0.3 mm with $u = 0.2, 0.5$ and 0.8 are shown in Fig. 7. The smaller the arc length s (or the curvature) is, the higher the interpolation accuracy is. Additionally, the d -curve appears pluses at $u \sim 0.25$ and ~ 0.75 . This results from the cusps of NURBS curves of the NURBS surface.

3.3 The Application of BEM-TRC

The simulation results based on Vericut software with and without BEM-TRC are shown in Fig. 8. The digital model in simulation is generated by fitting point cloud model. The maximum and average fitting error is 0.0707 mm and 0.0086 mm, respectively. The over-cut analysis error is set to be 0.071 mm. As can be observed in Fig. a and b, the milling effects without and with BEM-TRC are very good. However, there are large over-cut regions (red regions) without BEM-TRC as shown in Fig. 8a. Contrarily, when BEM-TRC is used, the over-cut phenomenon is avoided successfully as shown in Fig. 8b, and undercut regions appear. Fortunately, the undercut can be decreased using smaller radius BEMs. Table 1 outlines various model volumes with and without BEM-TRC. The volume of the digital model is 92,370.2015 mm³. The over-cut volume without BEM-TRC is -152.3945 mm³, while the residual volume with BEM-TRC is 283.8702 mm³. Figure 8a, b and Table 1 show that BEM-TRC can avoid over-cut phenomenon.

In order to verify the algorithm of BEM-TRC of NURBS surfaces, a part corresponding to Fig. 8b is machined based on a XK715D 3-axis CNC milling machine (Manufacturer: Hanchuan CNC Machine Tool Co., LTD, China) equipped with FANUC 0i-MB CNC system. Figure 9 displays the milling result of the part with BEM-TRC. Figures 8 and 9 demonstrate that the BEM-TRC algorithm proposed in this work is effective and feasible in the milling process of NURBS surfaces using BEMs for 3-axis CNC milling machines.

4 Conclusion/Recommendation

Aiming at 3-axis CNC milling machines with 2D-TRC for FEMs, a new TRC named BEM-TRC is presented in this work, and the relative algorithm for BEM-TRC is given. The BEM-TRC can realize the TRC function of NURBS surfaces when BEMs are used. The execution process can be divided into two steps as follows:

- (1) Search the cutting point on the NURBS surface using equi-arc length interpolation in u or v direction.
- (2) Fulfill BEM-TRC at a cutting point (CP) through offsetting the CP to the cutter center point (CCP) of a BEM along its normal vector.
- (3) The cutter location point (CLP) of the BEM can be calculated according to the BEM-CCP.

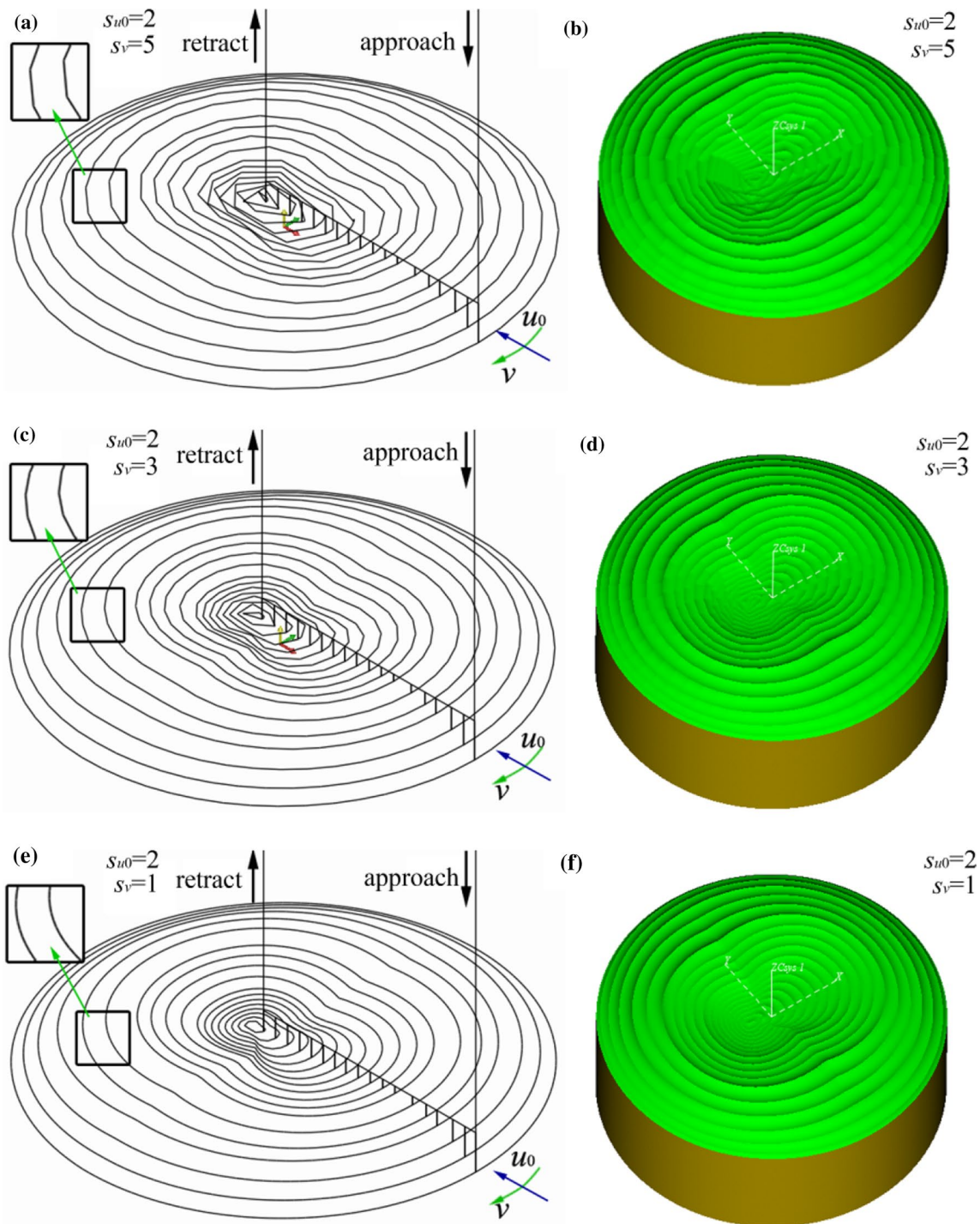


Fig. 4 The simulation results of EALI with BEM-TRC for a NURBS surface ($R=3$ mm). **a**, **c** and **e** The tool paths with $(s_{u0}, s_v)=(2, 5)$, $(2, 3)$ and $(2, 1)$, respectively. **b**, **d** and **f** The cutting effects with $(s_{u0}, s_v)=(2, 5)$, $(2, 3)$ and $(2, 1)$, respectively

A special toolbox based on Matlab software is obtained to execute the relative algorithm, and to generate CNC programs for FANUC CNC system. Using the toolbox, a

CNC milling program of a predefined NURBS surface corresponding to BEM-RC can be obtained for a 3-axis CNC milling machine.

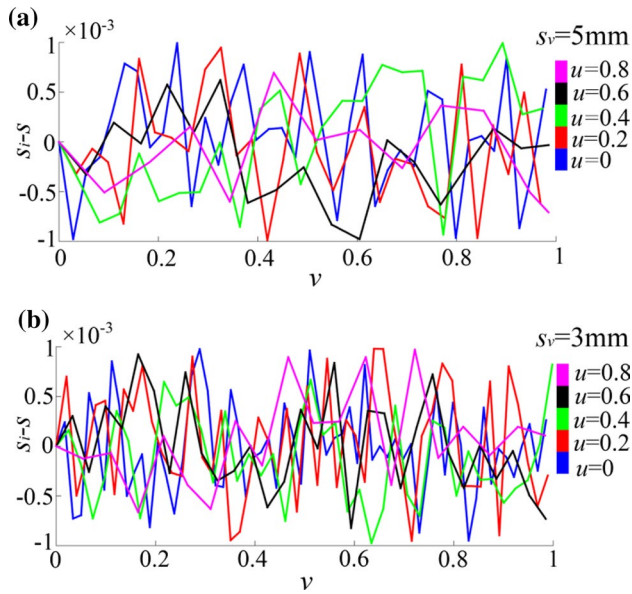


Fig. 5 The error of s_i-s in v direction of the NURBS surface, **a** $s_v=5$, **b** $s_v=3$

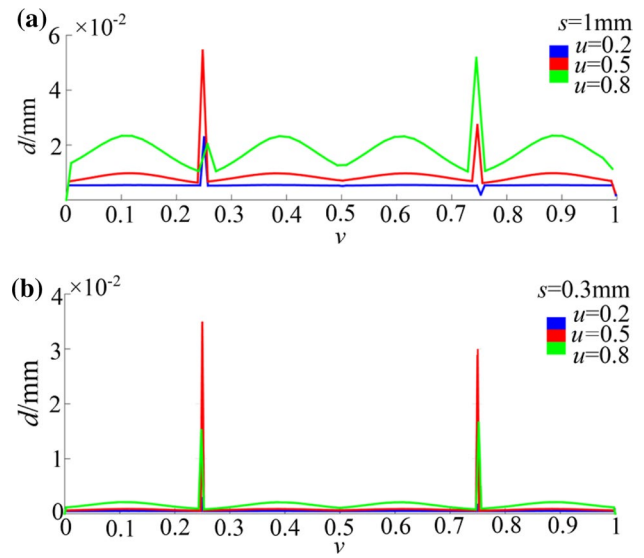


Fig. 7 The chord curves of various s values with $u=0.2, 0.5$ and 0.8 , **a** $s=1$ mm, **b** $s=0.3$ mm

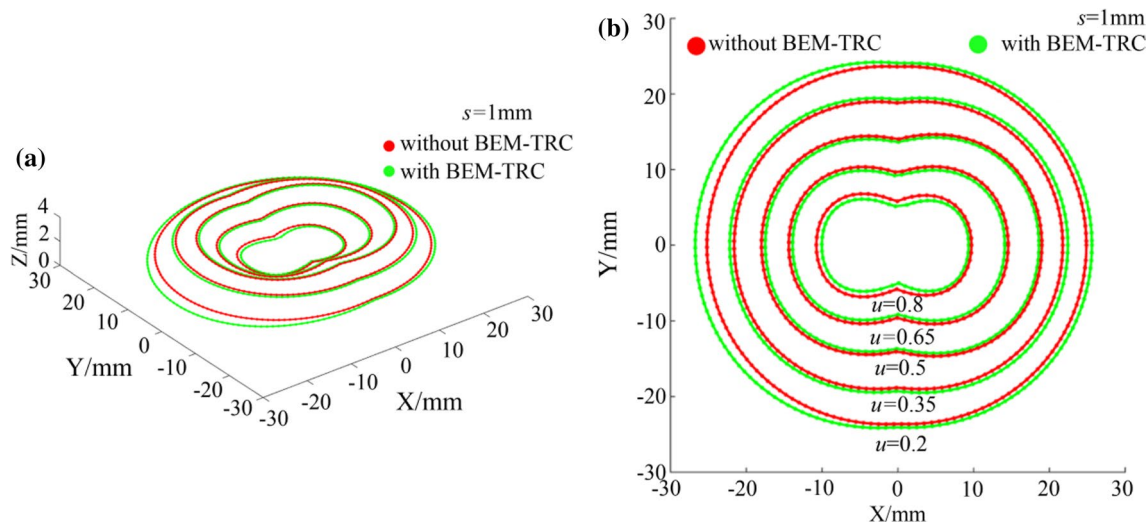


Fig. 6 The paths of the BEM-CLP with and without BEM-TRC ($R=3$ mm), **a** 3D-view, **b** XY view

The simulation based on the Vericut software and experiment based on a 3-axis CNC milling machine equipped with FANUC 0i-MB confirms that the BEM-TRC of NURBS surfaces is feasible and effective. The

BEM-TRC extends the 2D-TRC function of FEMs to BEMs, and makes 2D-TRC to be able to accomplish the milling of NURBS complex surfaces. The interpolation method with BEM-TRC can be applied to NURBS complex surfaces, and has broad application prospects for 3-axis CNC milling machines.

Fig. 8 The milling simulation results based on Vericut software with $s_{a0}=s_v=0.3$, **a**, **b** The over-cut check results without and with BEM-TRC, respectively. ($R=3$ mm, The red and blue denotes over-cut and undercut, respectively). (Color figure online)

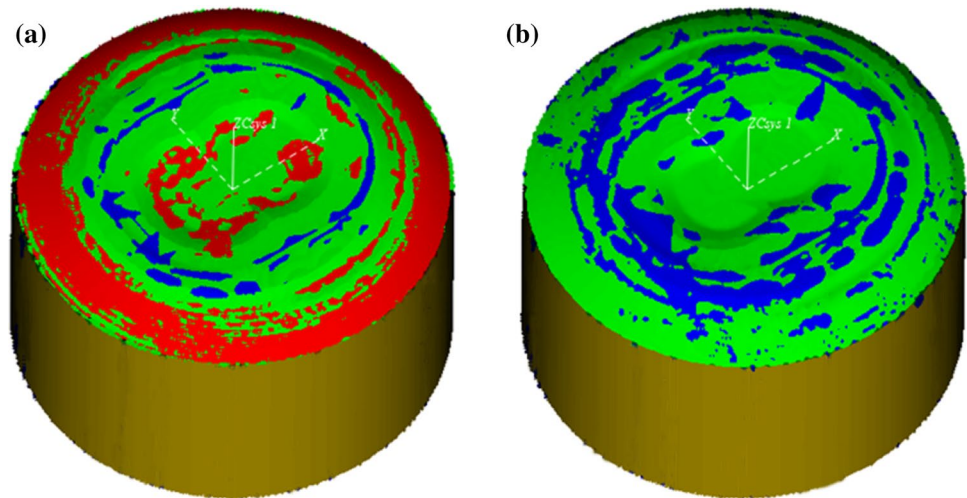
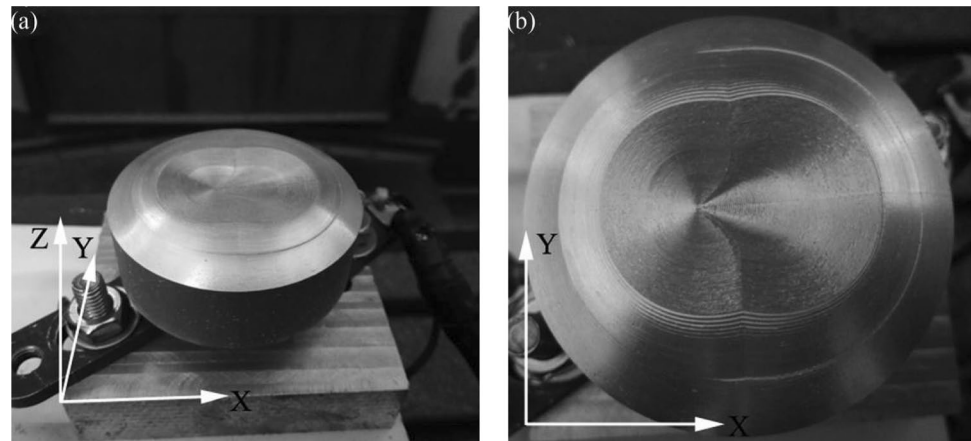


Table 1 The comparison of volumes with and without BEM-TRC

Model	Blank	Design model	Without BEM-TRC	With BEM-TRC
Volume (mm ³)	98,960.1686	92,370.2015	92,217.807	92,654.0717
Removed volume (mm ³)	–	–	6742.3616	6306.0969
Over-cut/Residual volume (mm ³)	–	–	– 152.3945	283.8702

Fig. 9 The milling results based on a 3-axis CNC milling machine ($R=3$ mm). **a** 3D-view. **b** XY view



Acknowledgements This project is supported by National Science and Technology Major Project (2017-VII-0003–0096-4, 2017-VII-0012–0108), National Natural Science Foundation of China (Grant no. 51764038 and 51465030), Gansu Science and Technology Planning Project (17YF1GA018, 17CX1JA117, and 18JR3RA132), Western Young Scholars of Chinese Academy of Sciences, Lanzhou Talent Innovation and Entrepreneurship Project (2019-RC-102 and 2018-RC-108), Longyuan Youth Innovative and Entrepreneurial Talents Project, Foundation of A Hundred Youth Talents Training Program of Lanzhou Jiaotong University, and Gansu Provincial Employee Technology Innovation Subsidy Fund Project.

Appendix A

The parameters of P , w , U , V , p and q for the NURBS surface shown in Fig. 2 are listed as follows. P is control point, w is weight, U and V are kont vectors, and p and q is degree.

$$P = \{ [30 \ 0 \ 0], [30 \ -30 \ 0], [0 \ -30 \ 0], [-30 \ -30 \ 0], [-30 \ 0 \ 0], [-30 \ 30 \ 0], [0 \ 30 \ 0], [30 \ 30 \ 0], [30 \ 0 \ 0]; [26 \ 0 \ 3], [26 \ -26 \ 3], [0 \ -26 \ 3], [-27 \ -27 \ 1], [-27 \ 0 \ 1], [-27 \ 27 \ 1], [0 \ 26 \ 3], [26 \ 26 \ 3], [26 \ 0 \ 3]; [24 \ 0 \ 3], [24 \ -24 \ 3], [0 \ -22 \ 3], [-24 \ -24 \ 3], [-24 \ 0 \ 3], [-24 \ 24 \ 3], [0 \ 22 \ 3], [24 \ 24 \ 3], [24 \ 0 \ 3];$$

[21 0 4], [21 -21 4], [0 -18 4], [-21 -21 4], [-21 0 4], [-21 21 4], [0 18 4], [21 21 4], [21 0 4]; [19 0 4], [19 -19 4], [0 -14 4], [-18 -18 4], [-18 0 4], [-18 18 4], [0 14 4], [19 19 4], [19 0 4]; [15 0 3.5], [15 -15 3.5], [0 -10 3.5], [-15 -15 3.5], [-15 0 3.5], [-15 15 3.5], [0 10 3.5], [15 15 3.5], [15 0 3.5]; [12 0 3], [12 -12 3], [0 -7 3], [-12 -12 3], [-12 0 3], [-12 12 3], [0 7 3], [12 12 3], [12 0 3]; [7 0 2], [7 -7 2], [0 -4 2], [-9 -9 2], [-9 0 2], [-9 9 2], [0 4 2], [7 7 2], [7 0 2]; [-5 0 2], [-5 0 2], [-5 0 2], [-5 0 2], [-5 0 2], [-5 0 2], [-5 0 2];

$w = [1 \ 0.707 \ 1 \ 0.707 \ 1 \ 0.707 \ 1 \ 0.707 \ 1; 1 \ 0.707 \ 1 \ 0.707 \ 1 \ 0.707 \ 1 \ 0.707 \ 1; 1 \ 0.707 \ 1 \ 0.707 \ 1 \ 0.707 \ 1 \ 0.707 \ 1; 1 \ 0.707 \ 1 \ 0.707 \ 1 \ 0.707 \ 1 \ 0.707 \ 1; 1 \ 0.707 \ 1 \ 0.707 \ 1 \ 0.707 \ 1 \ 0.707 \ 1; 1 \ 0.707 \ 1 \ 0.707 \ 1 \ 0.707 \ 1 \ 0.707 \ 1; 1 \ 0.707 \ 1 \ 0.707 \ 1 \ 0.707 \ 1 \ 0.707 \ 1; 1 \ 0.707 \ 1 \ 0.707 \ 1 \ 0.707 \ 1 \ 0.707 \ 1];$

$U = [0 \ 0 \ 0 \ 1/4 \ 1/4 \ 1/2 \ 1/2 \ 3/4 \ 3/4 \ 1 \ 1 \ 1];$

$V = [0 \ 0 \ 0 \ 1/4 \ 1/4 \ 1/2 \ 1/2 \ 3/4 \ 3/4 \ 1 \ 1 \ 1];$

$p = 2;$

$q = 2.$

References

- Chen, Z. C., & Fu, Q. (2007). A practical approach to generating steepest ascent tool-paths for three-axis finish milling of compound NURBS surfaces. *Computer-Aided Design*, 39(11), 964–974.
- Cheng, C.W., Tsa,i M.C., "Real-time variable feed rate NURBS curve interpolator for CNC machining," Int. J Adv. Manuf. Tech., Vol. 23, No. 11–12, pp. 865–873, 2004.
- Li, Y., Chen, W., Cai, Y., Nasri, A., & Zheng, J. (2015). Surface skinning using periodic T-spline in semi-NURBS form. *Journal of Computational and Applied Mathematics*, 273, 116–131.
- Ridwan, F., Xu, X., & Liu, G. (2010). A framework for machining optimisation based on STEP-NC. *Journal of Intelligent Manufacturing*, 23, 423–441.
- Xu, X. W. (2006). Realization of STEP-NC enabled machining. *Robotics and Computer-Integrated Manufacturing*, 22(2), 144–153.
- Lai, Y.-L. (2010). Tool-path generation of planar NURBS curves. *Robotics and Computer-Integrated Manufacturing*, 26(5), 471–482.
- Wang, Z. Q., & Wang, X. R. (2014). The principle and application of cutting-point virtual tool radius compensation for ellipsoidal outer contour finishing using a ball end mill. *The International Journal of Advanced Manufacturing Technology*, 71(9–12), 1527–1537.
- Yang, D. C. H., & Han, Z. (1999). Interference detection and optimal tool selection in 3-axis NC machining of free-form surfaces. *Computer Aided Design*, 3, 303–315.
- Yd, C., Hx, W., & Tm, W. (2011). Three-dimensional tool radius compensation for a 5-axis peripheral milling. *Advanced Science Letters*, 26(4), 3093–3096.
- Han, L., Gao, X. S., & Li, H. (2013). Space cutter radius compensation method for free form surface end milling. *The International Journal of Advanced Manufacturing Technology*, 67, 2563–2575.
- Haitao, H., Dong, Y., Lixian, Z., & Han, L. (2009). Research on 3D Cutter Radius Compensation for 5-Axis End Milling. *Chinese Journal of Mechanical Engineering*, 15, 1770–1774.
- Chu, Z. Y., Ahn, I. H., & Seung, K. (2017). Process monitoring and inspection systems in metal additive manufacturing: Status and applications. *International Journal of Precision Engineering and Manufacturing-Green Technology*, 4(5), 235–245.
- Park, D. H., & Kwon, H. H. (2016). Development of automobile engine mounting parts using hot-cold complex forging technology. *International Journal of Precision Engineering and Manufacturing-Green Technology*, 3(2), 179–184.
- Park, H. S., Dang, X. P., Nguyen, D. S., & Kumar, S. (2020). Design of advanced injection mold to increase cooling efficiency. *International Journal of Precision Engineering and Manufacturing-Green Technology*, 7(2), 319–328.
- Chu, C.-H., Wu, P.-H., & Lei, W.-T. (2010). Tool path planning for 5-axis flank milling of ruled surfaces considering CNC linear interpolation. *Journal of Intelligent Manufacturing*, 23(3), 471–480.
- Lin, B.-T., & Kuo, C.-C. (2009). Application of an integrated RE/ RP/CAD/CAE/CAM system for magnesium alloy shell of mobile phone. *Journal of Materials Processing Technology*, 209(6), 2818–2830.
- Park, K., Kim, Y. S., Kim, C. S., & Park, H. J. (2007). Integrated application of CAD/CAM/CAE and RP for rapid development of a humanoid biped robot. *Journal of Materials Processing Technology*, 187–188, 609–613.
- Campatelli, G., Scippa, A., Lorenzini, L., & Sato, R. (2015). Optimal workpiece orientation to reduce the energy consumption of a milling process. *International Journal of Precision Engineering and Manufacturing-Green Technology*, 2(1), 5–13.
- Lorenzo-Yustos, H., Lafont, P., Diaz Lantada, A., Navidad, A. F.-F., et al. (2010). Towards complete product development teaching employing combined CAD-CAM-CAE technologies. *Computer Applications in Engineering Education*, 18(4), 661–668.
- Piegl, L., & Tiller, W. (2012). *The NURBS Book*. Berlin: Springer.
- Wang, Y. S., Wang, X. R., Wang, Z. Q., Lin, T. S., & He, P. (2017). Preparation and microstructure of AlCoCrFeNi high-entropy alloy complex curve coatings. *Materials Science and Technology*, 33(5), 559–566.
- Wang, X. R., Wang, Z. Q., Wang, Y. S., Lin, T. S., & He, P. (2017). A bisection method for the milling of NURBS mapping projection curves by CNC machines. *The International Journal of Advanced Manufacturing Technology*, 91(1–4), 155–164.

Publisher's Note Springer Nature remains neutral with regard to jurisdictional claims in published maps and institutional affiliations.



Zhaoqin Wang is the associate professor in Lanzhou Jiaotong University and received her master's degree in Shenyang Ligong University in 2008. She is now pursuing her Ph.D. at Lanzhou University of Technology. Her research interests are robotic technologies, novel materials and surface modification. In recent year, she has published more than 15 papers.



Xiaorong Wang is the professor and doctoral supervisor in Lanzhou Jiaotong University and received his Ph.D degree in Harbin Institute of Technology in 2017. He preside over more than 20 projects from NSFC, Gansu Science and Technology Planning Project, Lanzhou Talent Innovation and Entrepreneurial Talents Project and so on. He has published more than 15 papers in journals such as *J. Mater. Eng. Perform.*, *Int. J. Adv. Manuf. Tech.* and *Mater. Sci. Eng. A*. His research interests include

CNC technologies, robotics, advanced processing, welding, surface modification and novel materials.



Yusen Wang was the graduate student in Lanzhou Jiaotong University and received his master's degree in 2017. His research interests are CNC technologies, NURBS theory and CNC programming.



Ruijun Wang is the researcher and doctoral supervisor, and received a Ph.D degree in Harbin Institute of Technology in 2005. He is currently the director of the Institute of new material technology and equipment of CAAMS, the chief engineer / deputy general manager of Beijing JinLunKunTian Special Machinery Co., Ltd., and the chief expert of CNMIC and CAAMS. In 2016, he was entitled to the State-Council Allowance Obtained Expert. He is a member of the expert group of the major consulting project of “strategic research on material longevity and sustainable development” of Chinese Academy of engineering, expert of the professional group of “two machine special basic research” of the Ministry of industry and information technology, project review expert of the Ministry of science and technology, vice president of China Association of Machinery Manufacturing Technology, director of Chinese Society of Rare Earths, chairman of materials and manufacturing branch of Chinese Society for Agricultural Machinery, and Zhongguancun material test technology Vice president of the alliance, part-time professor of State Key Laboratory of Advanced Welding and Joining (Harbin Institute of Technology), Xi'an Jiaotong University,

and external researcher of Ningbo Institute of Materials Technology & Engineering, CAS. His research focuses on additive manufacturing direction in the field of material processing engineering. He has presided over and completed a number of national major projects, won one first prize of national technology invention, one first prize of national defense technology invention and two second prizes of national defense technology invention, obtained more than 20 authorized patents, cultivated 11 doctoral and master's graduates, and won the national “outstanding engineer Award” in 2018.

Manyu Bao is a master of engineering, senior engineer, deputy director of advanced surface technology research and development center of Beijing JinLunKunTian Special Machinery Co., Ltd., and deputy secretary general of materials and manufacturing technology branch of Chinese Society for Agricultural Machinery. For a long time, she has been engaged in the technical research on the application and performance evaluation of high reliability material surface engineering technology in the complex service environment of special equipment. She is responsible for a number of major national security basic research projects, military supporting scientific research projects of science and Industry Bureau, and two special projects of Ministry of industry and information technology.




Tiesong Lin received a Ph.D degree from Harbin Institute of Technology in 2009. He is currently professor and doctoral supervisor of State Key Laboratory of Advanced Welding and Joining, Harbin Institute of Technology. He presided over more than 30 projects from NSFC, National Key R&D Program of China and so on. He has published more than 90 academic papers in journal such as *J. Am. Ceram. Soc.*, *J. Eur. Ceram. Soc.* and *Scripta Marer*. His research interests include advanced joining of ceramic/metal, brazing and diffusion bonding of dissimilar materials, glass package and solid-state battery.



Peng He is a professor and doctoral supervisor of Harbin University of technology. At present, he is vice president of School of materials science and engineering, Harbin University of technology, and vice director of State Key Laboratory of Advanced Welding and Joining. His research direction is the mechanism of special welding



Springer 

metallurgy and the regulation of microstructure and performance. He has presided over more than 30 projects at all levels, such as national key research and development plan, national 973, 863 and national natural fund. The research achievements include one second prize of

National Natural Science, one second prize of national science and technology progress, one first prize of Natural Science Award of Ministry of education, two outstanding awards of Chinese patent, etc. He has published or co published 160 papers.